Substitution and Redox Chemistry of $[Bu_4N]_2[Ta_6Cl_{12}(OSO_2CF_3)_6]$

Nicholas Prokopuk, Vance O. Kennedy, Charlotte L. Stern, and Duward F. Shriver*

Department of Chemistry, Northwestern University, Evanston, Illinois 60208-3113

Received March 24, 1998

Two sequential electrochemical reductions occur for the cluster anion $[Ta_6Cl_{12}(OSO_2CF_3)_6]^{2-}$ at 0.89 and 0.29 V vs Ag/AgCl, with the generation $[Ta_6Cl_{12}(OSO_2CF_3)_6]^{3-}$ and $[Ta_6Cl_{12}(OSO_2CF_3)_6]^{4-}$. Chemical reduction of $[Ta_6Cl_{12}(OSO_2CF_3)_6]^{2-}$ by ferrocene produces $[Ta_6Cl_{12}(OSO_2CF_3)_6]^{3-}$ with the concomitant shift of the $\nu(SO_2)$ stretch from 1002 to 1018 cm^{-1}. Reaction of $[Bu_4N]_2[Ta_6Cl_{12}(OSO_2CF_3)_6]$ (**1**) with $[Bu_4N]X$ (X = Cl, Br, I, NCS) occurs by reduction and substitution, yielding $[Bu_4N]_3[Ta_6Cl_{12}X_6]$, where the clusters with X = Br, I, and NCS are new. Spectroscopic (IR and UV−vis) evidence indicates that the reduced cluster core $\{Ta_6Cl_{12}\}^{2+}$ is produced in reaction mixtures of **1** with the halide and pseudohalide ions. Concomitant substitution of the triflate ligands of **1** by X^- occurs and the rates for the overall reduction and substitution increase in the order $X^- = Cl^- < Br^- < NCS^- < I^- < CN^-$. Reduction of **1** with ferrocene followed by addition of $[Bu_4N]O_2CCH_3$ produces the new cluster $[Ta_6Cl_{12}(O_2CCH_3)_6]^{3-}$ isolated as the tetrabutylammonium salt. Cyclic voltammetry and UV−vis spectroscopy on the new clusters $[Bu_4N]_3[Ta_6Cl_{12}X_6]$ (X = Br, I, NCS, and O_2CCH_3) are reported. Crystal data for $[Bu_4N]_3[Ta_6Cl_{12}(NCS)_6]\cdot CH_2Cl_2$: monoclinic, space group, $P2_1/c$ (No. 14); $a = 25.855(6)$ Å, $b = 21.843(6)$ Å, $c = 16.423(3)$ Å; $\beta = 100.03(2)°$; $V = 9133(3)$ Å^3; $Z = 4$.

Introduction

Hexanuclear cluster compounds of the early transition metals with halide ligands adopt two common structural motifs: $[M_6Y_8X_6]^{2-}$ and $[M_6Y_{12}X_6]^{(6-n)-}$. Clusters of the group 6 metals Mo and W have the former composition and the group 5 metals Nb and Ta have the latter. One notable exception is the electron deficient cluster $Nb_6I_8(NH_2CH_3)_6$ which has face-bridging iodide ligands.[1] All of these clusters consist of an octahedral arrays of metal atoms with either eight face capping or twelve edge-bridging inner halide ligands, Y. Six outer (axial) ligands, X, are terminally bound one to each metal center as shown in Figure 1. The inner ligands, Y, are substitutionally inert, while the axial ligands are somewhat more labile. The introduction of weakly coordinating ligands such as triflate[2−4] (trifluoromethanesulfonate, $OSO_2CF_3^-$), tetrafluoroborate,[5−9] nitrate,[7,10,11] acetonitrile,[12] or trifluoroacetate[13] at the axial positions increases the substitutional lability of these sites. The triflate derivative $[Bu_4N]_2[Mo_6Cl_8(OSO_2CF_3)_6]$ has proven to be a versatile starting material for new metal halide clusters in which the $Mo_6Cl_8^{4+}$ core is retained, and we recently reported the preparation and characterization of the analogous $[Bu_4N]_2[Ta_6Cl_{12}(OSO_2CF_3)_6]$.[2,4]

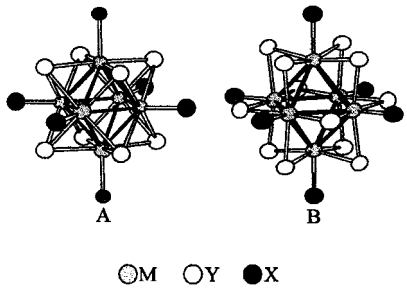

Figure 1. Structures of $[M_6Y_8X_6]^z$ **A** and $[M_6Y_{12}X_6]^z$ **B**.

The niobium and tantalum metal halide clusters exhibit an extensive redox chemistry and five different oxidation states are electrochemically accessible over the range $[M_6Y_{12}X_6]^{5-}$ to $[M_6Y_{12}X_6]^{1-}$ where X is an anionic ligand and the charge on the cluster core $\{M_6Y_{12}\}^{n+}$ ranges from $n = 1$ to 5.[14−18] In the present discussion it is convenient to refer to the charge of only the $\{M_6Y_{12}\}^{n+}$ unit instead of the entire cluster and its full complement of axial ligands $[M_6Y_{12}X_6]^{(6-n)-}$. This notation is especially useful when there is ambiguity as to the type and charge of the ligand occupying the axial sites. The average

(1) Stollmaier, F.; Simon, A. *Inorg. Chem.* **1985**, *24*, 168−171.
(2) Johnston, D. H.; Gaswick, D. C.; Lonergan, M. C.; Stern, C. L.; Shriver, D. F. *Inorg. Chem.* **1992**, *31*, 1869−1873.
(3) Johnston, D. H.; Stern, C. L.; Shriver, D. F. *Inorg. Chem.* **1993**, *32*, 5170−5175.
(4) Kennedy, V. O.; Stern, C. L.; Shriver, D. F. *Inorg. Chem.* **1994**, *33*, 5967−5969.
(5) Harder, K.; Peters, G.; Preetz, W. *Z. Anorg. Allg. Chem.* **1991**, *598/599*, 139−149.
(6) Preetz, W.; Harder, K.; Schnering, H. G. v.; Kliche, G.; Peters, K. *J. Alloys Compd.* **1992**, *183*, 413−429.
(7) Preetz, W.; Dublitz, D.; Schnering, H. G. v.; Sassmannshausen, J. *Z. Anorg. Allg. Chem.* **1994**, *620*, 234−246.
(8) Brückner, P.; Peters, G.; Preetz, W. *Z. Anorg. Allg. Chem.* **1993**, *619*, 551−558.
(9) Brückner, P.; Peters, G.; Preetz, W. *Z. Anorg. Allg. Chem.* **1993**, *619*, 1920−1926.
(10) Bublitz, D.; Preetz, W.; Simsek, M. K. *Z. Anorg. Allg. Chem.* **1997**, *623*, 1−7.
(11) Simsek, M. K.; Preetz, w. *Z. Anorg. Allg. Chem.* **1997**, *623*, 515−523.
(12) Ehrlich, G. M.; Warren, C. J.; Haushalter, R. C.; DiSalvo, F. J. *Inorg. Chem.* **1995**, *34*, 4284−4286.
(13) Harder, K.; Preetz, W. *Z. Anorg. Allg. Chem.* **1992**, *612*, 97−100.
(14) Klendworth, D. D.; Walton, R. A. *Inorg. Chem.* **1981**, *20*, 1151−1155.
(15) Pénicaud, A.; Batail, P.; Coulon, C.; Canadell, E.; Perrin, C. *Chem. Mater.* **1990**, *2*, 123−132.
(16) Quigley, R.; Barnard, P. A.; Hussey, C. L.; Seddon, R. *Inorg. Chem.* **1992**, *31*, 1255−1261.
(17) Hussey, C. L.; Quigley, R.; Seddon, K. R. *Inorg. Chem.* **1995**, *34*, 370−377.
(18) Cooke, N. E.; Kuwana, T.; Espenson, J. *Inorg. Chem.* **1971**, *10*, 1081−1083.

S0020-1669(98)00334-6 CCC: $15.00
Published on Web 08/20/1998

oxidation states of the individual metal atom ranges from 2.17 for $\{M_6Y_{12}\}^{1+}$ to 2.83 for $\{M_6Y_{12}\}^{5+}$. A series of clusters $\{M_6Y_{12}\}^{n+}$ ($n = 2-4$) with both neutral and anionic axial ligands have been structurally characterized and only small changes in M−M bond lengths are observed over this range of oxidation states.[19] The electron donor strength of the axial ligand influences the substitutional lability of these sites and the stability of the various oxidation states of the cluster. Phosphine ligands, which are π-acceptors, stabilize the lower oxidation states, and the π-donor chloride ligand stabilizes the higher oxidation states.[14,19] Electronic spectra for the $n = 4$ and $n = 3$ states of the $\{Ta_6Cl_{12}\}^{n+}$ core are similar and this may lead to confusion in assigning the particular electronic transitions of the clusters as it is difficult to recognize mixtures of oxidation states.[19−22] In both oxidation states the tantalum clusters produce orange-brown to yellow solutions. The more reduced $n = 2$ species is easily identified by a large increase in absorption in the visible region of the spectrum, resulting in solutions with a dark green color.

In the present work we report on the reactions of $[Bu_4N]_2[Ta_6Cl_{12}(OSO_2CF_3)_6]$, **1**, with ligands that are potential reductants. Substituted clusters with the general formula $[Ta_6Cl_{12}X_6]^{3-/4-}$ are formed. Metathesis reactions between **1** and the anionic ligands are generally accompanied by a redox process. The charge of the substituted product is found to vary with the electrochemical properties of the anionic ligand. The crystal structure of one of these new mixed ligand clusters, $[Bu_4N]_3[Ta_6Cl_{12}(NCS)_6]$, was determined in the present study.

Experimental Section

Apparatus. IR spectra were obtained with a Bomem MB-100 FTIR spectrometer with 2-cm^{-1} resolution on solutions in 0.1 mm path length CaF_2 solution cells or on Nujol mulls between KBr plates. UV−vis spectra were obtained on a Cary 1E UV−vis spectrophotometer in 1.0 cm path length fused-quartz cells equipped with a valve to exclude air. Mass spectra were obtained at the Midwest Center for Mass Spectrometry (University of Nebraska, Lincoln) or the Analytical Services Laboratory at Northwestern University. Elemental analysis were preformed by Elbach Analytical Laboratories (Gummersbach, Germany) or Oneida Research Services, Inc. (Whitesboro, NY). Energy dispersive spectrometry were preformed with a Hitachi S4500 field emission scanning electron microscope equipped with a Noran Voyager X-ray detector system.

Cyclic voltammograms were obtained with a Bioanalytical Systems 100B electrochemical analyzer. A Pt-disk working electrode and a Pt-foil counter electrode were employed in a single-compartment cell. The reference electrode for these experiments was a commercial (BAS) Ag/AgCl electrode, which was separated from the bulk solution by a porous Vycor tip. All electrochemical experiments were preformed at room temperature in dry nitrogen purged cells with degassed solvents and recrystallized $[Bu_4N]BF_4$ (Aldrich) from methanol/diethyl ether.

Materials. The solvents dichloromethane, tetrahydrofuran, diethyl ether, and acetonitrile were dried over P_2O_5, sodium benzophenone, sodium benzophenone, or CaH_2, respectively, and distilled prior to use. $[Bu_4N]X$ (X = Br, I, CN, NCS, O_2CCH_3) were used as received from Aldrich. $[Bu_4N]Cl$ (Aldrich) was recrystallized from methanol and diethyl ether. Ferrocene (Aldrich) was sublimed before use. $[Bu_4N]_2[Ta_6Cl_{12}(OSO_2CF_3)_6]$ was synthesized from $[Bu_4N]_2[Ta_6Cl_{12}Cl_6]$ and triflic acid, $HOSO_2CF_3$, as previously described.[4] Trimethylsilyl triflate, $(CH_3)SiOSO_2CF_3$, and methyl triflate, $CH_3OSO_2CF_3$, were sometimes used in place of triflic acid for the synthesis of $[Bu_4N]_2[Ta_6Cl_{12}(OSO_2CF_3)_6]$, **1**.

Reaction of 1 with Cp_2Fe. Two stock solutions (28 mg of **1** in 30 mL and 5 mg Cp_2Fe in 5 mL of CH_2Cl_2) were prepared. Aliquots (5 mL) of the cluster solution were combined with varying amounts of the ferrocene solution. Reactions were monitored by infrared and UV−visible spectroscopy.

Reaction of 1 with X^- (X = Cl, Br, I, CN, NCS, O_2CCH_3). To a stirred solution of **1** (50 mg, 0.017 mmol) in 10 mL of CH_2Cl_2 or THF under a nitrogen atmosphere was added a solution of a tetrabutylammonium salt containing one of the anions Cl^-, Br^-, I^-, CN^-, NCS^-, or $O_2CCH_3^-$ (0.138 mmol in 10 mL of solvent). Progress of the reaction was monitored by IR and UV−visible spectroscopy.

Synthesis of $[Bu_4N]_3[Ta_6Cl_{12}X_6]$ (X = Cl, Br, I). Under a nitrogen atmosphere, solid **1** (50 mg, 0.017 mmol) and 0.136 mmol of the tetrabutylammonium salt were combined in a Schlenk flask and dissolved in 20 mL of CH_2Cl_2. The flask was connected to a water-cooled condenser with a mineral oil bubbler, the resulting solution was refluxed for 48 h (X = Cl), 45 h (X = Br), or 12 h (X = I) and then filtered. The filtrate was concentrated to ca. 2 mL under vacuum and diethyl ether was added dropwise until formation of a brown-orange precipitate was complete. The solid product was isolated by vacuum filtration, washed with a 5 mL portion of diethyl ether, and dried under vacuum. The yield for X = Cl was 51%. Anal. Calcd for $C_{48}H_{108}N_3Cl_{18}Ta_6$: C, 23.52; H, 4.44; N, 1.71. Found: C, 22.80; H, 4.14; N, 1.74. The yield for X = Br was 42%. Anal. Calcd for $C_{48}H_{108}N_3Br_6Cl_{12}Ta_6$: C, 21.21; H, 4.01; N, 1.55. Found: C, 21.54; H, 3.91; N, 1.60. The yield for X = I was 42%. Anal. Calcd for $C_{48}H_{108}N_3Cl_{12}I_6Ta_6$: C, 19.22; H, 3.63; N, 1.40. Found: C, 17.98; H, 3.16; N, 1.40. Calcd for $C_{48}H_{108}N_3Cl_{12}I_6Ta_6 + 2CH_2Cl_2$: C, 18.95; H, 3.56; N, 1.33. Elemental analysis for the iodo and acetate derivatives are low in carbon by 1.2%. Some oxidized cluster $[Bu_4N]_2[Ta_6Cl_{12}X_6]$, X = I or O_2CCH_3, present in less than 10% may account for the discrepancy. The presence of the oxidized cluster may not be apparent in the absorption spectra owing to the similarity in the spectra of clusters in the $n = 3$ and $n = 4$ oxidation.

Synthesis of $[Bu_4N]_3[Ta_6Cl_{12}(NCS)_6]$. Under nitrogen, a solution of **1** (108 mg, 0.0374 mmol) in 6 mL of CH_2Cl_2 was added dropwise to a solution containing $[Bu_4N][NCS]$ (0.339 mmol in 10 mL of CH_2Cl_2). The resulting mixture was stirred in the absence of light for 1 day, filtered, and layered with diethyl ether (5 mL). The yellow-brown crystals were determined to be the $[Bu_4N]^+$ salts of $[Ta_6Cl_{12}(NCS)_6]^{3-}$. Yield for $[Bu_4N]_3[Ta_6Cl_{12}(NCS)_6]$ 52%. IR (CH_2Cl_2, cm^{-1}): 2068 (ν(CN)). Anal. Calcd for $C_{54}H_{108}Cl_{12}N_9S_6Ta_6$: C, 25.07; H, 4.21; N, 4.87; Cl, 16.45; Ta, 41.97. Found C, 24.52; H, 4.63; N, 4.92; Cl, 16.14; Ta, 41.20.

$[Bu_4N]_3[Ta_6Cl_{12}(O_2CCH_3)_6]$. A 112 mg (0.039 mmol) sample of **1** and $(C_5H_5)_2Fe$ (14.5 mg, 0.078 mmol) were combined in a Schlenk flask under nitrogen and dissolved in 10 mL of CH_2Cl_2. A solution of $[Bu_4N][O_2CCH_3]$ (104 mg, 0.35 mmol in 10 mL of CH_2Cl_2) was added dropwise and the resulting mixture was allowed to stir overnight. The volume was reduced to 2 mL, and the concentrated solution was layered with 8 mL of degassed diethyl ether under a nitrogen atmosphere. The resulting red-brown solid was isolated by filtration and washed with Et_2O. The yield of $[Bu_4N]_3[Ta_6Cl_{12}(O_2CCH_3)_6]$, 66.6 mg, was 66%. IR ($CH_2Cl_2$, cm^{-1}): 1624 (ν(C═O)), 1364 (ν(C−O)). Anal. Calcd for $C_{60}H_{126}N_3O_{12}Cl_{12}Ta_6$: C, 27.79; H, 4.90; N, 1.62. Found C, 26.52; H, 4.83; N, 1.23. Calcd. for $C_{60}H_{126}N_3O_{12}Cl_{12}Ta + CH_2Cl_2$: C, 27.36; H, 4.82; N, 1.57.

X-ray Structure Determination of $[Bu_4N]_3[Ta_6Cl_{12}(NCS)_6]\cdot 2CH_2Cl_2$. Crystals were obtained from a concentrated CH_2Cl_2 solution which was carefully layered with diethyl ether under nitrogen and set aside for several weeks in the absence of light. A brown-yellow single crystal (0.44 × 0.43 × 0.03 mm) was selected from a homogeneous collection of crystals, immersed in Paratone-N (Exxon) oil, mounted on a glass fiber and transferred to the nitrogen cold stream of an Enraf-Nonius CAD-4 diffractometer with graphite monochromated Mo Kα radiation. Cell constants and an orientation matrix for data collection were obtained from a least squares refinement of the setting angles of 25 carefully centered reflections ($20.0 < 2\theta < 23.5°$). Based on the systematic absences of *h 0 l* ($l = 2n + 1$) and *0 k 0* ($k = 2n + 1$) and the successful solution and refinement of the structure, the space group was determined to be $P2_1/c$ (No. 14). The data were collected (−*h*,

(19) Imoto, H.; Hayakawa, S.; Morita, N.; Saito, T. *Inorg. Chem.* **1990**, *29*, 2007−2014.
(20) Schneider, R. F.; Mackay, R. A. *J. Chem. Phys.* **1968**, *48*, 843−851.
(21) Fleming, P. B.; McCarley, R. E. *Inorg. Chem.* **1970**, *9*, 1347−1354.
(22) Robbins, D. J.; Thomson, A. J. *J. Chem. Soc., Dalton Trans.* **1972**, 2350−2364.

Table 1. Crystallographic Data for $[Bu_4N]_3[Ta_6Cl_{12}(NCS)_6]\cdot 2CH_2Cl_2$

empirical formula	$C_{54}H_{108}Cl_{12}N_9S_6Ta_6\cdot 2CH_2Cl_2$
fw	2756.86
cryst syst	monoclinic
space group	$P2_1/c$ (No. 14)
a, Å	25.855(6)
b, Å	21.843(6)
c, Å	16.423(3)
β, deg	100.03(2)
V, Å^3	9133(3)
Z	4
λ(Å)	0.710 73
d_{calcd}, g/cm^3	2.005
μ (Mo Kα), cm^{-1}	77.90
radiation	Mo Kα (λ = 0.710 69 Å)
temp, °C	−120
R^a	0.043
$R_w{}^b$	0.038

^{a} $\sum||F_o| - |F_c||/\sum|F_o|$. ^{b} $[\sum w(|F_o| - |F_c|)^2/\sum w|F_o|^2]^{1/2}$.

$+k, \pm l$ at −120 ± 1 °C using an $\omega-\theta$ scan to a maximum 2θ of 45.9°. A total of 13 383 reflections were measured of which 13 114 were considered unique (R_{int} = 0.216) and 7144 ($I > 3.00\sigma(I)$) and these were utilized in the structure determination. A summary of relevant crystallographic data is provided in Table 1. The intensities of three representative reflections were measured after every 90 min of X-ray exposure, and these remained constant throughout the data collection. The data were corrected for Lorentz and polarization effects. An analytical absorption correction was applied which resulted in transmission factors ranging from 0.08 to 0.56.

All calculations were carried out with the Texsan crystallographic software package of Molecular Structure Corporation.[23] The structure was solved by direct methods[24] and expanded using Fourier techniques.[25] Neutral atom scattering factors were taken from the literature.[26] Anomalous dispersion effects were included in F_{calc}.[27] The values for $\Delta f'$ and $\Delta f''$ were those of Creagh and McAuley.[28] Mass attenuation coefficients were those of Creagh and Hubbel.[29] The carbon atoms on the cluster and the C48a and C48b atoms, which were assigned half occupancy, were refined isotopically. C48a and C48b were refined with group isotropic thermal parameters. The remaining non-hydrogen atoms were refined anisotropically. Hydrogen atoms were included in fixed positions but not refined. The final cycle of full-matrix least-squares refinement[30] included 808 variable parameters and converged (largest parameter shift was 0.73 times its esd) to an R value of 0.043 (R_w = 0.038). The standard deviation of an observation of unit weight[31] was 1.75. The weighting scheme was based on counting statistics and included a factor (p = 0.006) to down weight the intense reflections.

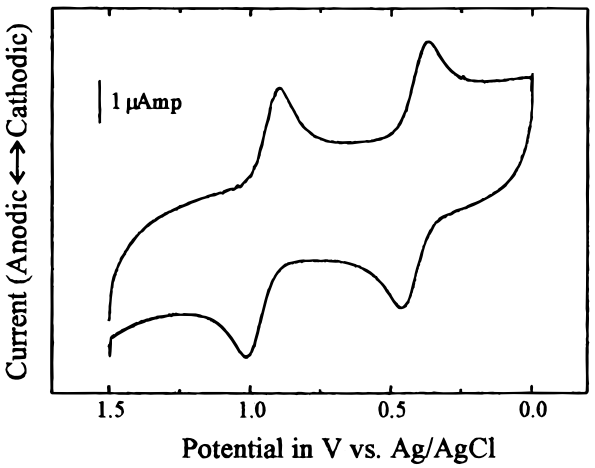

Figure 2. Cyclic voltammogram of $[Bu_4N]_2[Ta_6Cl_{12}(OSO_2CF_3)_6]$ in a 0.1 M solution of $[Bu_4N]BF_4$ in CH_2Cl_2 with a scan rate of 100 mV/s and Pt working and counter electrodes.

Plots of $\sum w(|F_o| - |F_c|)^2$ versus $|F_o|$, reflection order in data collection, sin θ/λ, and various classes of indices showed no unusual trends. The maximum and minimum peaks on the final difference Fourier map corresponded to 1.59 and −1.49 e/Å^3, respectively, and were in the vicinity of the tantalum positions.

Results and Discussion

Reduction of $[Bu_4N]_2[Ta_6Cl_{12}(OSO_2CF_3)_6]$. Cyclic voltammetry of $[Bu_4N]_2[Ta_6Cl_{12}(OSO_2CF_3)_6]$ in a CH_2Cl_2 solution of 0.1 M $[Bu_4N]BF_4$ reveal two one-electron reduction waves at 0.89 and 0.29 V vs Ag/AgCl, corresponding to the generation of $[Ta_6Cl_{12}(OSO_2CF_3)_6]^{3-}$ and $[Ta_6Cl_{12}(OSO_2CF_3)_6]^{4-}$, respectively, Figure 2. Infrared spectra of **1** dissolved in 0.1 M $[Bu_4N]BF_4$ methylene chloride solution indicate that the triflate ligands remain coordinated to the $\{Ta_6Cl_{12}\}^{4+}$ core of **1** in this electrolyte solution. The reduction potentials of $[Ta_6Cl_{12}(OSO_2CF_3)_6]^{2-}$ and $[Ta_6Cl_{12}(OSO_2CF_3)_6]^{3-}$ are the most positive observed for clusters containing the $\{Ta_6Cl_{12}\}^{3+/4+}$ core and attest to the poor electron donor properties of the triflate ligand. Both redox couples of **1** are chemically reversible in CH_2Cl_2 or CH_3CN electrolytes with no new waves appearing on the voltammograms after repeated cycles. In contrast $[Ta_6Cl_{12}Cl_6]^{4-}$ undergoes facile substitution of an axial Cl^- ligand by a CH_3CN molecule.[17] The resistance of $[Ta_6Cl_{12}(OSO_2CF_3)_6]^{4-}$ toward substitution of the axial triflate ligands by acetonitrile is attributed to the weak donor properties of $OSO_2CF_3{}^-$. Apparently, the reduced $\{Ta_6Cl_{12}\}^{+2}$ core is stabilized by the low electron donor character of triflate. By contrast, the chloride ligand which is a stronger σ- and π-donor is not strongly bonded to the reduced metal core as indicated by the displacement of Cl^- by the neutral electron donor acetonitrile. Peak separations ΔE_p for **1**, ∼70 mV, are consistent with a minimal structural change during the redox processes. Both redox couples display linear plots of $\nu^{1/2}$ vs i characteristic of a diffusion-controlled process.[32]

The $\nu(SO_3)$ bands of the coordinated triflate ligand are useful for monitoring reactions of **1**. Reduction of the symmetry of $OSO_2CF_3{}^-$ upon coordination leads to a total of three IR-active SO_3 stretching frequencies, compared to two for the free ion. The SO_3 bands observed for **1** in CH_2Cl_2 occur at 1350, 1205, and 1002 cm^{-1}. Assignment of the SO_3 stretches was based on the detailed analysis of the analogous cluster $[Bu_4N]_2[Mo_6$-

(23) *Texsan, Crystal Structure Analysis Package*; Molecular Structure Corporation: The Woodlands, TX, 1985 and 1992.
(24) Sheldrick, G. M. SHELXS86. In *Crystallographic Computing 3*; Sheldrick, G. M., Kruger, C., Goddard, R., Eds.; Oxford University Press: Oxford, 1985; pp 175−189.
(25) DIRDIF92: Beurskens, P. T.; Admiral, G.; Beurskens, G.; Bosman, W. P.; Garcia- Granda, S.; Gould, R. O.; Smits, J. M. M.; Smykalla, C. *The DIRDIF program system: Direct methods for difference structure factors*; Technical Report of the Crystallography Laboratory: University of Nijmgegen, The Netherlands, 1992.
(26) Cromer, D. T.; Waber, J. T. *International Tables for X-ray Crystallography*; The Kynoch Press: Birmingham, England, 1974; Vol. IV.
(27) Ibers, J. A.; Hamilton, W. C. *Acta Crystallog.* **1964**, *17*, 781.
(28) Creagh, D. C.; McAuley, W. J. *International Tables for Crystallography*; Kluwer Academic Publishers: Boston, 1992; Vol. C.
(29) Creagh, D. C.; Hubbell, J. H.; *International Tables for X-ray Crystallography*; Wilson, A. J. C., Ed.; Kluwer Academic Publishers: Boston, 1992; Vol. C Table 2.3.4.3, pp 200−206.
(30) Least-squares: The function minimized was $\sum w(|F_o| - |F_c|)^2$, where: $w = 4F_o^2/\sigma^2(F_o^2)$ and $\sigma^2(F_o^2) = [S^2(C + R^2B) + (pF_o^2)^2]/Lp^2$ (S = scan rate, C = total integrated peak count, R = ratio of scan time to background counting time, B = total background count, Lp = Lorentz−polarization factor, and p = p factor).
(31) Standard deviation of an observation of unit weight: $[\sum w(|F_o| - |F_c|)^2/(N_o - N_v)]^{1/2}$, where N_o = number of observations and N_v = number of variables.
(32) Bard, A. J.; Faulkner, L. R. *Electrochemical Methods Fundamentals and Applications*; John Wiley & Sons: New York, 1980.

$Cl_8(OSO_2CF_3)_6]$.[2] Reduction of an orange solution of $[Ta_6Cl_{12}(OSO_2CF_3)_6]^{2-}$ with 1 equiv of Cp_2Fe shifts two of the SO_3 bands from 1350 to 1335 cm^{-1} and from 1002 to 1018 cm^{-1}. No change in the $\nu(SO_3)$ region is observed with further addition of ferrocene; however, a visible color change from the characteristic orange of the $\{Ta_6Cl_{12}\}^{3+/4+}$ clusters to light green occurs, indicating the presence of the more-reduced $\{Ta_6Cl_{12}\}^{2+}$ core. From the reduction potentials of **1** and Cp_2Fe, the reduction of $[Ta_6Cl_{12}(OSO_2CF_3)_6]^{2-}$ by ferrocene is expected to stop at $[Ta_6Cl_{12}(OSO_2CF_3)_6]^{3-}$ as the IR data indicates. The light green color is attributed to the high molar absorptivity of reduced $\{Ta_6Cl_{12}\}^{2+}$ clusters,[19,33] which accentuates the detection of trace amounts of $[Ta_6Cl_{12}(OSO_2CF_3)_6]^{4-}$.

Reaction of 1 with X^- (X = Cl, Br, I, CN, NCS, O_2CCH_3). The positive reduction potentials of $[Ta_6Cl_{12}(OSO_2CF_3)_6]^{2-}$ indicate that this cluster is a relatively strong oxidizing agent. The substitutional lability of **1** toward various anionic ligands increases with the ease of oxidation of the ligand and therefore its tendency to reduce the cluster. Chloride, the weakest reducing agent of the series, reacts slowly with **1**. After 24 h of refluxing **1** with a 8-fold excess of $[Bu_4N]Cl$ in CH_2Cl_2, four $\nu(SO_3)$ bands are observed at 1335, 1205, 1031, and 1018 cm^{-1}. The SO_3 bands at 1335, 1205, and 1018 cm^{-1} indicate the presence of the reduced cluster $[Ta_6Cl_{12}(OSO_2CF_3)_6]^{3-}$, and the band at 1031 cm^{-1} indicates the presence of uncoordinated (free) triflate.[2,34] Although two SO_3 stretches are expected in the IR spectra for the free triflate ion, only the symmetric $\nu(SO_3)$ stretch is observed at 1031 cm^{-1} in methylene chloride, due to overlap of the asymmetric band with those of the solvent. A single SO_3 stretch at 1031 cm^{-1} is observed after the reaction mixture was refluxed for 48 h, indicating the formation of the fully substituted cluster $[Bu_4N]_3[Ta_6Cl_{12}Cl_6]$. From the reduction potentials of **1** and Cl_2 (1.29 V vs Ag/AgCl in CH_2Cl_2, 0.1 M in $[Bu_4N]BF_4$) the cluster should not be reduced by chloride; however, refluxing **1** in CH_2Cl_2 in the absence of Cl^- does not produce any change in the $\nu(SO_3)$ region. This precludes the solvent or the tetrabutylammonium counterions as the reducing agent and suggests that the chloride anion is in fact acting as the reductant. A solution to this dilemma is that a slow stream of nitrogen was passed over the vessel used to reflux the reaction mixture and this may promote the loss of Cl_2. In keeping with this interpretation, iodide−starch paper placed at the top of the condenser darkened as the reaction progressed, indicating a strong oxidizing agent was produced by the refluxing mixture. Energy dispersive spectrometry confirmed the presence of chloride on the paper exposed to the reaction mixture while paper not exposed to the reaction mixture showed no evidence for chloride. Thus, we must conclude that Cl^- is acting as the reductant in the reaction mixture. Hussey and co-workers attributed the decomposition of $[Nb_6Cl_{12}Cl_6]^{2-}$ to $[Nb_6Cl_{12}Cl_6]^{3-}$ in Lewis basic chloroaluminate melts to a similar homogeneous reduction by chloride ions.[16] An alternative source of the reduced clusters $[Ta_6Cl_{12}(OSO_2CF_3)_6]^{3-}$ is disproportionation of **1** into mononuclear Ta(V) species and reduced triflate clusters, $[Ta_6Cl_{12}(OSO_2CF_3)_6]^{3-/4-}$. Since only a trace amount of cluster would have to be sacrificed as Ta(V), the mononuclear complex may remain undetected. This explanation is consistent with the observations only if the disproportionation reaction is facilitated by the anions.

In contrast with chloride, the cyanide anion reacts rapidly with **1**. Addition of an 8-fold excess of $[Bu_4N]CN$ to **1** in CH_2Cl_2 results in an dark green solution, with an infrared band at 1031 cm^{-1}, $\nu(SO_3)$, and three CN stretches at 2120, 2158, and 2192 cm^{-1}, shifted from 2055 cm^{-1} for free cyanide. The multiple $\nu(CN)$ stretching frequencies are consistent with the presence of more than one oxidation state, $[Ta_6Cl_{12}(CN)_6]^{(6-n)-}$, and the intense green color can be attributed to a substantial concentration of the reduced $\{Ta_6Cl_{12}\}^{2+}$ core arising from reduction by CN^-. Reduction potentials of CN^- and **1** are consistent with this interpretation. Mass spectrometry indicates all of the triflate ligands were replaced by cyanide (FAB-MS *m*/*z* calcd (obsd) for $[Bu_4N]_2[Ta_6Cl_{12}(CN)_6]^-$: 2152 (2151)). The cyclic voltamogram contains two clean reduction waves, described below, indicating the presence of one type of metal cluster complex in solution. Elemental analysis (high in C, H, and N for $[Bu_4N]_3[Ta_6Cl_{12}(CN)_6]$) and the multiple $\nu(CN)$ bands, however, indicate that a mixture of oxidation states is present in the solid product.

Mixtures of **1** with I^-, Br^-, $O_2CCH_3^-$, or NCS^- in CH_2Cl_2 undergo color changes from orange to green and back to orange over the course of the reaction. The intensity of the green color correlates with the reducing character of the anionic ligand. In reaction mixtures of **1** with an 8-fold excess of NCS^- four $\nu_s(SO_3)$ bands are observed at 1002, 1018, 1026, and 1031 cm^{-1} in the region of the symmetric stretch of free triflate (990−1035 cm^{-1}) as the reaction progresses. The previously unobserved SO_3 band at 1026 cm^{-1} may arise from the fully reduced $[Ta_6Cl_{12}(OSO_2CF_3)_6]^{4-}$ cluster or a partially triflate substituted analogue. Full substitution of the triflate ligands occurs for X = Br^-, I^-, and NCS^- when an 8-fold excess of ligand is used. UV−vis spectra and elemental analysis of the isolated products indicate a 3− charge for $[Bu_4N]_3[Ta_6Cl_{12}X_6]$ with the $\{Ta_6Cl_{12}\}^{3+}$ core. Reaction of **1** with 8 equiv of $O_2CCH_3^-$ does not lead to the expected cluster $[Bu_4N]_3[Ta_6Cl_{12}(O_2CCH_3)_6]$, but addition of $O_2CCH_3^-$ to a solution containing **1** and Cp_2Fe in a 1:2 molar ratio leads to $[Ta_6Cl_{12}(O_2CCH_3)_6]^{3-}$. Apparently the prior reduction of **1** by ferrocene facilitates the clean substitution of acetate for triflate ions.

The observed rates of the substitution reaction between **1** and various anions increases with the series $Cl^- < Br^- < NCS^- < I^- < CN^-$. This trend does not correlate with basicity or the polarizability of the anions, and it suggests other factors influence the redox/substitution process. The observed trend is consistent with a rate dependence on the oxidation potentials of the anions X^-. This correlation of oxidation potentials with reaction rates is expected if reduction of **1** to $[Ta_6Cl_{12}(OSO_2CF_3)_6]^{3-}$ is required prior to substitution.

A sequence for the redox/substitution reactions of **1** with the various reducing ligands is shown in Scheme 1. Surprisingly, the simple metathesis reaction **A** is not observed for any of the anions used for this study. Even the strong π-electron donor Cl^- does not displace the triflate ligands of **1**, but upon refluxing **1** with Cl^- reduction and concomitant Cl^- substitution for triflate occur. With the more easily oxidized anions reduction steps **B** and **C** are readily accessible and generation of the reduced triflate species $[Ta_6Cl_{12}(OSO_2CF_3)_6]^{3-/4-}$ provides two possible routes to the substituted products $[Ta_6Cl_{12}X_6]^{3-}$. The intense green color of the reaction mixture which is characteristic of the reduced cluster $[Ta_6Cl_{12}X_6]^{4-}$ provides evidence for the pathway through steps **D** and **E**. Further, evidence for the reduction steps stems from reactions of **1** with 6 equiv of the anionic ligands X^-. Similar color changes occur in these reaction mixtures, indicating that a redox process takes place similar to reactions of **1** with 8 equiv of X^-, however, in reactions of **1** with only 6 equiv of ligand, incomplete substitu-

(33) Espenson, J. H.; McCarley, R. E. *J. Am. Chem. Soc.* **1966**, *88*, 1063−1064.
(34) Johnston, D. H.; Shriver, D. F. *Inorg. Chem.* **1993**, *32*, 1045−1047.

Scheme 1

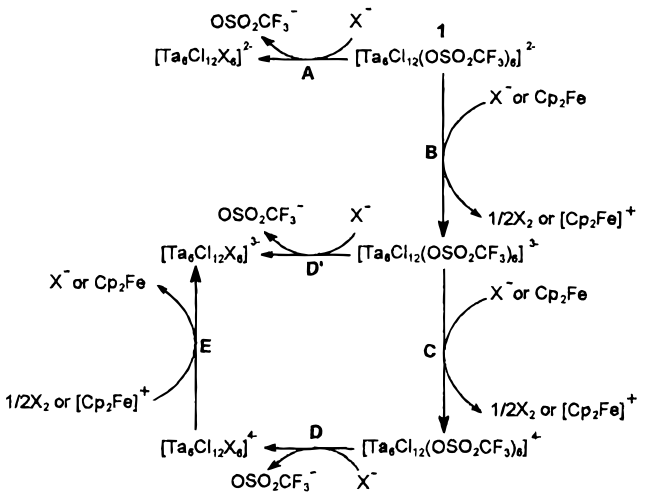

Table 2. UV−Vis Absorption Data for $[Bu_4N]_3[Ta_6Cl_{12}X_6]$[a]

cluster	λ (nm)
$[Bu_4N]_3[Ta_6Cl_{12}Cl_6]$	245, 284, 360, 445, 875
$[Bu_4N]_3[Ta_6Cl_{12}Br_6]$	247, 281, 361, 435, 532, 853
$[Bu_4N]_3[Ta_6Cl_{12}I_6]$	243, 292, 373, 443, 567, 839
$[Bu_4N]_3[Ta_6Cl_{12}(O_2CCH_3)_6]$	222, 286, 350, 737, 880
$[Bu_4N]_3[Ta_6Cl_{12}(NCS)_6]$	225, 256, 275, 358, 434, 751, 861

[a] All spectra obtained in CH_3CN.

tion of the triflate ligands occurs indicating the consumption of X^- in the reduction of **1**. The possibility that methylene chloride is the sole oxidizing agent in step **E** was eliminated when reaction mixtures of **1** and the ligands in dry THF underwent a color change similar to those observed in CH_2Cl_2 solution. In reactions of **1** with the more reducing CN^- ligand, a mixture of the two different oxidation states of the reduced product is obtained $[Ta_6Cl_{12}(CN)_6]^{3-/4-}$. Ferrocene acts as the reducing agent in steps **B** and **C** and ferrocenium is the reoxidizing agent, step **E**, in the reaction of **1** with $O_2CCH_3^-$. For all cases reduction of **1** is proposed as the initial step, followed by displacement of the triflate ligands. The possibility of initial substitution of the triflate ligands of **1** by X^- to generate $[Ta_6Cl_{12}X_6]^{2-}$ which is then followed by reduction to $[Ta_6Cl_{12}X_6]^{3-}$ cannot be ruled out; however, the reduction potentials of **1** and the substituted clusters $[Ta_6Cl_{12}X_6]^{2-}$ make the reaction sequence of Scheme 1 more plausible.

Characterization of $[Bu_4N]_3[Ta_6Cl_{12}X_6]$ (X = Br, I, NCS, O_2CCH_3). Electronic absorption maxima for the new clusters are given in Table 2. The oxidation states of the $\{Ta_6Cl_{12}\}^{n+}$ clusters cannot be assigned with confidence based solely on UV−vis spectroscopy,[19−22] but the correlation of absorption spectra with elemental analysis establish that $n = 3$ $\{Ta_6Cl_{12}\}^{n+}$ for the new clusters. Cyclic voltammograms for the new clusters, where X = CN, Br, NCS, and O_2CCH_3, reveal two chemically reversible redox waves. These electron-transfer reactions correspond to generation of the $[Ta_6Cl_{12}X_6]^{2-}$ and $[Ta_6Cl_{12}X_6]^{4-}$ and half-wave potentials obtained in 0.1 M $[Bu_4N]BF_4-CH_2Cl_2$ are given in Table 3. Peak separations ΔE_p for the redox couples of the bromide and thiocyanate derivatives are between 60 and 90 mV, consistent with reversible or quasireversible electron-transfer processes. Both the acetate and cyanide derivatives have large ΔE_p values (>120 mV). Cyclic voltammograms for the iodide cluster exhibit two chemically irreversible waves at 0.50 and 0.80 V verses Ag/AgCl. With the acetate and bromide clusters a third redox couple is observed corresponding to formation of $[Ta_6Cl_{12}X_6]^-$, which contains the $\{Ta_6Cl_{12}\}^{5+}$ core, seen previously only in the all chloro clusters $[Ta_6Cl_{12}Cl_6]^-$.[17]

Table 3. $E_{1/2}$ Values (in V) for $[Bu_4N]_3[Ta_6Cl_{12}X_6]$ Clusters in CH_2Cl_2

compound	$E_{1/2}$ (ox)	$E_{1/2}$ (red)
$[Bu_4N]_3[Ta_6Cl_{12}(CN)_6]$	0.43[a]	−0.23[a]
$[Bu_4N]_3[Ta_6Cl_{12}(NCS)_6]$	0.35	−0.10
$[Bu_4N]_3[Ta_6Cl_{12}Br_6]$	1.10, 0.14	−0.36
$[Bu_4N]_3[Ta_6Cl_{12}(O_2CCH_3)_6]$	1.15, −0.11[a]	−0.54[a]

[a] Irreversible electron transfers in CH_2Cl_2 (ΔE_p values greater than 120 mV at scan rates of 100 mV/s). Potentials are determined from CV experiements in 0.1 M $[Bu_4N]BF_4$.

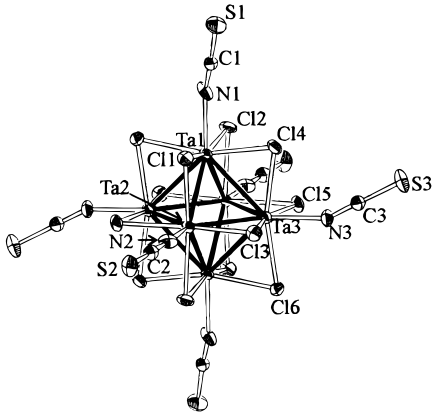

Figure 3. Diagram of one anion in the crystal structure of $[Bu_4N]_3[Ta_6Cl_{12}(NCS)_6]\cdot 2CH_2Cl_2$. Thermal ellipsoids are at 50% probability.

Single-crystal X-ray diffraction on a brown-yellow crystal of $[Bu_4N]_3[Ta_6Cl_{12}(NCS)_6]$ reveals a unit cell containing two independent half-anions, three $[Bu_4N]^+$ cations, and two CH_2Cl_2 solvent molecules. Each anionic cluster $[Ta_6Cl_{12}(NCS)_6]^{3-}$ is situated on an inversion center, and half of the atoms are related by the center of symmetry. Both anions are essentially identical; the X-ray data for the anion containing Ta(1), Ta(2), and Ta(3) are discussed, while data for the second anion are presented in parentheses where appropriate. Figure 3 shows the $[Ta_6Cl_{12}(NCS)_6]^{3-}$ cluster unit. The Ta_6 core is a slightly distorted octahedron, in agreement with the essentially octahedral metal array in other $[Ta_6Cl_{12}X_6]^{3-}$ systems.[19,35−37] The average Ta−Ta bond length, 2.93 Å (2.93 Å), agrees with that expected for a $[Ta_6Cl_{12}X_6]^{3-}$ core. The nearest-neighbor Ta−Cl distances range from 2.426 to 2.462 Å (2.437−2.458 Å). The narrow Ta−Ta−Ta angles range from 59.68 to 60.29° (59.58−60.23°), while the wide angles range from 89.68 to 90.32° (89.76−90.24°). The NCS^- groups are bound with the nitrogen end to tantalum and the average Ta−N bond length is 2.15 Å (2.15 Å). The NCS^- ligands are almost linear with an average N−C−S angle of 178° (178°) and are bound in a slightly bent fashion relative to tantalum as evidenced by the average Ta−N−C angle of 159° (165°). The atomic coordinates and *B*(eq) values are given in Table 4, while Table 5 lists selected bond distances and angles for the cluster.

The CN stretching frequency in the infrared spectrum of $[Ta_6Cl_{12}(NCS)_6]^{3-}$ occurs at 2068 cm^{-1}, which is higher than the value 2054 cm^{-1} for free NCS^-. This 14 cm^{-1} frequency shift to higher energy contrast with the observations for

(35) Bauer, D.; Schnering, H. G. *Z. Anorg. Allg. Chem.* **1968**, *361*, 259−277.
(36) Brničevič, N.; Ružič-Toroš, Ž.; Kojič-Prodic, B. *J. Chem. Soc., Dalton Trans.* **1985**, 455−458.
(37) Brničevič, N.; Nöthig-Hus, D.; Kojič-Prodic, B.; Ružič-Toroš, Ž.; Danilovič, Ž.; McCarley, R. E. *Inorg. Chem.* **1992**, *31*, 3924−2928.

Table 4. Selected Interatomic Distances (Å) and Bond Angles (deg) for $[Bu_4N]_3[Ta_6Cl_{12}(NCS)_6]\cdot 2CH_2Cl_2$

Ta(1)−Ta(2)	2.928(1)	Ta(2)−Cl(1)	2.445(5)
Ta(1)−Ta(2′)	2.922(1)	Ta(2)−Cl(2′)	2.459(4)
Ta(1)−Ta(3)	2.932(1)	Ta(2)−Cl(3)	2.446(5)
Ta(1)−Ta(3′)	2.930(1)	Ta(2)−Cl(5′)	2.427(3)
Ta(1)−Cl(1)	2.460(5)	Ta(2)−N(2)	2.17(2)
Ta(1)−Cl(2)	2.460(5)	Ta(3)−Cl(3)	2.450(5)
Ta(1)−Cl(4)	2.426(5)	Ta(3)−Cl(4)	2.436(4)
Ta(1)−Cl(6′)	2.462(5)	Ta(3)−Cl(5)	2.451(5)
Ta(1)−N(1)	2.15(1)	Ta(3)−Cl(6)	2.454(4)
Ta(2)−Ta(3)	2.927(1)	Ta(3)−N(3)	2.13(2)
Ta(2)−Ta(3′)	2.940(1)	S(1) −C(1)	1.61(2)
S(2) −C(2)	1.56(2)	S(3) −C(3)	1.65(2)
Ta(4)−Ta(5)	2.939(1)	Ta(5)−Cl(8′)	2.440(4)
Ta(4)−Ta(5′)	2.915(1)	Ta(5)−Cl(9)	2.444(5)
Ta(4)−Ta(6)	2.928(1)	Ta(5)−Cl(10)	2.452(5)
Ta(4)−Ta(6′)	2.934(1)	Ta(5)−Cl(12′)	2.454(6)
Ta(4)−Cl(7)	2.458(5)	Ta(5)−N(5)	2.15(2)
Ta(4)−Cl(8)	2.439(5)	Ta(6)−Cl(7)	2.457(4)
Ta(4)−Cl(10)	2.449(6)	Ta(6)−Cl(9)	2.437(5)
Ta(4)−Cl(11′)	2.447(5)	Ta(6)−Cl(11)	2.453(4)
Ta(4)−N(4)	2.17(1)	Ta(6)−Cl(12)	2.446(5)
Ta(5)−Ta(6)	2.935(1)	Ta(6)−N(6)	2.18(2)
Ta(5)−Ta(6′)	2.932(1)	S(4) −C(4)	1.60(2)
S(5)−C(5)	1.61(2)	S(6)−C(6)	1.59(2)
N(1)−C(1)	1.17(2)	N(2)−C(2)	1.20(2)
N(3)−C(3)	1.16(2)	N(4)−C(4)	1.17(2)
N(5)−C(5)	1.17(2)	N(6)−C(6)	1.16(2)

Ta(1)−Ta(2′)−Ta(3)	60.13(3)	Ta(1)−Ta(3′)−Ta(2)	59.85(3)
Ta(1)−Ta(2′)−Ta(3′)	60.02(3)	Ta(1)−Ta(3′)−Ta(2′)	59.85(3)
Ta(3)−Ta(2)−Ta(3′)	90.22(3)	Ta(2)−Ta(3)−Ta(2′)	89.78(3)
Ta(2)−Ta(1)−Ta(3′)	60.24(3)	Ta(3)−Ta(1)−Ta(3′)	90.32(3)
Ta(2)−Ta(1′)−Ta(3)	60.29(3)	Ta(2)−Ta(1′)−Ta(3′)	60.02(3)
Ta(2)−Ta(1)−Ta(2′)	90.09(3)	Ta(2)−Ta(1)−Ta(3)	59.92(3)
Ta(4)−Ta(5)−Ta(4′)	89.90(3)	Ta(4)−Ta(6)−Ta(4′)	89.76(3)
Ta(4)−Ta(5)−Ta(6)	59.80(3)	Ta(4)−Ta(6)−Ta(5)	60.17(3)
Ta(4)−Ta(5)−Ta(6′)	59.96(3)	Ta(4)−Ta(6)−Ta(5′)	59.67(3)
Ta(4)−Ta(5)−N(5)	133.0(4)	Ta(4)−Ta(6)−N(6)	135.0(4)
Ta(2)−Ta(3′)−N(3′)	134.3(5)	Ta(3)−Ta(2′)−N(2′)	134.1(5)
Ta(4)−Ta(5′)−N(5′)	137.1(4)	Ta(4)−Ta(6′)−N(6′)	135.2(4)
S(1)−C(1)−N(1)	177(2)	Ta(1)−N(1)−C(1)	155(2)
S(2)−C(2)−N(2)	178(2)	Ta(2)−N(2)−C(2)	168(2)
S(3)−C(3)−N(3)	179(2)	Ta(3)−N(3)−C(3)	153(1)
Ta(4)−N(4)−C(4)	175(1)	S(4)−C(4)−N(4)	178(2)
Ta(5)−N(5)−C(5)	160(2)	S(5)−C(5)−N(5)	179(2)
Ta(6)−N(6)−C(6)	159(2)	S(6)−C(6)−N(6)	178(2)

$[Mo_6Cl_8(NCS)_6]^{2-}$ where the two ν(CN) bands shift by 13 and 35 cm^{-1} to lower energy. The NCS^- ligands of $[Mo_6Cl_8(NCS)_6]^{2-}$ are also nitrogen bound as determined by IR,[38] ^{15}N NMR,[13] and X-ray crystallography.[39] The average M−N−C angle for the molybdenum cluster is 171° versus 162° for the tantalum cluster. Kinematic arguments predict that the CN frequency will be higher for the more linear M−N−C angle.[40] Bailey *et al.*[41] have found that the ν(CN) bands of N-bound thiocyanate complexes are virtually independent of the mass of the metal atom. Thus, it is unlikely that the observed shift to higher energy arises from the high mass of the tantalum atoms offsetting the lower M−N−C angle. Reduction of $[Ta(NCS)_6]^{2-}$ to $[Ta(NCS)_6]^{3-}$ shifts the ν(CN) from 2020 to 2110 cm^{-1} concomitant with a decrease in the Ta−N−C angle.[42−44] Similar trends in the ν(CN) and M−N−C angle of the molybdenum and the tantalum bound thiocyanate ligands likely reflect increased electron density on the metal centers of $[Ta_6Cl_{12}(NCS)_6]^{3-}$. The observed changes in the ν(CN) band are in the opposite direction to that predicted by kinematic or π-back-bonding effects[41] suggesting other factors are influencing the ν(CN) frequency.

The MS-FAB$^-$ data of $[Bu_4N]_3[Ta_6Cl_{12}(NCS)_6]$ show a complex parent peak envelope with a maximum *m*/*z* of 2585.3 amu, which agree well ($R = 8.0\%$ over a *m*/*z* range of 2581.3−2591.3) for the calculated peak envelope. Two intense ions in the spectrum are assigned as $[Bu_4N]_2[Ta_6Cl_{12}(NCS)_6]$ (*m*/*z*, found 2343.2; calcd 2344.5) and $[Bu_4N][Ta_6Cl_{12}(NCS)_6]$ (*m*/*z*, found 2101.0; calcd 2101.1). Fragments resulting from NCS and Cl loss were also observed. A rather unexpected fragment corresponds to loss of S from the NCS group indicating transformation of a nitrogen-bound NCS to −NC or possibly −CN.

Conclusions

Owing to the positive reduction potentials of $[Bu_4N]_2[Ta_6Cl_{12}(OSO_2CF_3)_6]$ the $\{Ta_6Cl_{12}\}^{4+}$ core is reduced by anions such Cl^-, Br^-, I^-, NCS^-, CN^-, and $O_2CCH_3^-$. This process was utilized to synthesize the new clusters $[Bu_4N]_3[Ta_6Cl_{12}X_6]$ (X = Br, I, NCS, O_2CCH_3) from **1** and an excess of the ligand X^-. Cyclic voltammetry on the two new cluster derivatives X = Br and $O_2CCH_3^-$ suggest the presence of a rarely observed $\{Ta_6Cl_{12}\}^{5+}$ core, previously seen only in $[Ta_6Cl_{12}Cl_6]^-$. The present work provides a systematic procedure to generate new clusters with the $\{Ta_6Cl_{12}\}^{3+}$ core having a variety of axial ligands.

Acknowledgment. We gratefully appreciate the National Science Foundation, Grant No. CHE-9417250, for funding and the Nebraska Center for Mass Spectrometry for MS-FAB$^-$ analysis.

Supporting Information Available: Tables of position parameters, thermal parameters, bond distances, bond angles, and atomic coordinates are available for $[Bu_4N]_3[TaCl_2(NCS)_6]\cdot 2CH_2Cl_2$ (20 pages). X-ray crystallographic files, in CIF format, are also available on the Internet only. Ordering and access information is given on any current masthead page.

IC980334D

(38) Weissenhorn, v. R. G. *Z. Anorg. Allg. Chem.* **1976**, *426*, 159−172.
(39) Guirauden, A.; Johannsen, I.; Batail, P.; Coulon, C. *Inorg. Chem.* **1993**, *32*, 2446−2452.
(40) Bignozzi, C. A.; Argazzi, R.; Schoonover, J. R.; Gordon, K. C.; Dyer, R. B.; Scandola, F. *Inorg. Chem.* **1992**, *31*, 5260−5267.
(41) Bailey, R. A.; Kozak, S. L.; Michelsen, T. W.; Mills, W. N. *Coord. Chem. Rev.* **1971**, *6*, 407−445.
(42) Schwochau, K.; Astheimer, L.; Schenk, H. J. *J. Inorg. Nucl. Chem.* **1973**, *35*, 2249−2257.
(43) Trop, H. S.; Davison, A.; Jones, A. G.; Davis, M. A.; Szalda, D. J.; Lippard, S. J. *Inorg. Chem.* **1980**, *19*, 1105−1110.
(44) Williams, G. A.; Bonnyman, J.; Baldas, J. *Aust. J. Chem.* **1987**, *40*, 27−33.